www.sensorsportal.com

Sensors & Transducers

Published by IFSA Publishing, S. L., 2019
http://www.sensorsportal.com

Study of Hydrogen Peroxide Vapors Sensor Made of Nanostructured Co-doped SnO_2 Film

[1] Vladimir AROUTIOUNIAN, [1] Valeri ARAKELYAN, [1] Mikayel ALEKSANYAN, [1] Gohar SHAHNAZARYAN, [1] Artak SAYUNTS and [2] Berndt JOOST

[1] Yerevan State University, Department of Physics of Semiconductors and Microelectronics,
1 A. Manoogian St., Yerevan, 0025, Republic of Armenia
[2] Institute for Pharmaceutical Technology, Fachhochschule Nordwestschweiz, Hochschule für Life Sciences,
Gründenstrasse 40, CH-4132 Muttenz, Switzerland
[1] Tel.: + 37460710311, fax: + 37460710355
[1] E-mail: kisahar@ysu.am

Received: 30 November 2018 /Accepted: 31 December 2018 /Published: 31 January 2019

Abstract: A technology was developed for manufacturing the hydrogen peroxide vapors solid-state semiconductor sensor. Gas sensitive nanostructured films made of doped metal oxide SnO_2<Co> were manufactured by the high-frequency magnetron sputtering method. The chemical composition of prepared SnO_2<Co> targets was analyzed. The thickness of the deposited doped metal oxide film was measured. The morphology of the deposited Co-doped SnO_2 film was studied by scanning electron microscopy. The sensor sensitivity to the different concentrations of hydrogen peroxide vapors was measured at different operating temperatures. It was found that the Co-doped SnO_2 sensor exhibit a sufficient sensitivity to very low concentration of hydrogen peroxide vapors (875 ppb) at the operating temperature of 100 °C. It exhibits a sensitivity at low operating temperature (25 °C) when exposed to hydrogen peroxide vapors with a concentration greater than 3.5 ppm. The optimal performance was observed at the operating temperature of 150 °C. The sensor made of SnO_2<Co> had potential application in real samples for the implementation of medical diagnostic apparatus for use in determining low concentration of hydrogen peroxide vapors.

Keywords: Sensor, Nanostructured film, Semiconductor, Doped metal oxide, Hydrogen peroxide vapors.

1. Introduction

Hydrogen peroxide (H_2O_2) is a colorless liquid, soluble with water in all proportions. It is unstable and can easily break down into water and oxygen producing energy. It is known as a good oxidizing agent and can cause spontaneous combustion when it comes in contact with organic material. In some cases, H_2O_2 or its vapors can be dangerous for human health. Brief contact of H_2O_2 with the skin leads to irritation and whitening. The extent of the hazard is determined by the concentration of the H_2O_2 solution. Contact with the eyes can lead to serious injury. Drinking a weak solution of H_2O_2 can cause severe gastrointestinal effects [1].

H_2O_2 (with a liquid and vapor form) has a wide application fields in different area. It can be used as an anti-bacterial agent in the medical field. It can be also used for disinfection and sterilization in everyday life and industry. It is utilized in chemical industry, in manufacturing organic products, mining industry for extraction uranium from ores, analytical chemistry, rocketry, bipropellant systems and so on.

As mentioned, H_2O_2 serves as a disinfectant for medical equipment and surfaces as well as for sterilizing of surgical instruments. The process of decontamination can be carried out in different ways: mechanical, chemical, physical, and physicochemical ways. The chemical decontamination which has many advantages, in turn, is divided into two groups: wet decontamination (water solution of ClO_2, H_2O_2, NaOCl and so on) and dry decontamination (vapor or gas phase of H_2O_2, ClO_2, O_3 and so on). The "ideal decontamination agent" should be not non-toxic to humans and environment, compatible with different materials, easily detectable and cheaper. The best candidate for "ideal decontamination agent" is the H_2O_2 vapor phase. It is able to sterilize a wide range of microorganisms. It has also high germicidal activity. The correct selection of the H_2O_2 concentration during the sterilization of the equipment and technological surfaces as well as a control of the H_2O_2 content in air after completion of disinfection cycle are very important. Therefore, the development and manufacturing of stable and reproducible sensors sensitive to H_2O_2 vapors are extremely required [2-9].

The near-infrared spectrophotometry was used for the monitoring of the concentration of H_2O_2 vapors in the course of the sterilization [10-12]. The chemiresistive films made from organic p-type semiconductors phthalocyanines metalized with elements of p-, d-, and f-blocks were also sensitive to H_2O_2 vapors [13-14].

There are many methods to detect and analyze different gases including gas chromatography, Fourier-transform infrared spectroscopy, chemiluminescence detectors, mass spectrometry, semiconductor gas sensors and so on. Solid-state gas sensors made from metal oxide semiconductors (MOSs) have many advantages in comparison to other gas sensing methods. These are used to monitor the content of oxidizing and reducing gas molecules in the environment. MOSs gas sensors have been widely studied due to their low costs, easy to miniaturize and production, high stability, reliability and can be designed to operate under different conditions including high temperatures, installation in small space and so on [15].

As the typical n-type MOS, tin oxide (SnO_2) with a wide band-gap (3.6 eV) has been widely used in *solid-state* gas sensors because of its low cost, non-toxicity, easy-achieved real-time response in gas-sensing application, low operating temperatures, high sensitivities and mechanical simplicity of sensor design, high reactivity to reducing gases at relatively low operating temperatures and easy adsorption of oxygen at its surface because of the natural non-stoichiometry. In the last 15 years, SnO_2 is considered the most widely used and studied material in the field of gas sensors. The conductivity of SnO_2 based sensor increases in the presence of a reducing gases, and decreases in the presence of an oxidizing gas. As a well-studied material gas-sensitive mechanisms related with adsorption/desorption processes as well as grains and pores sizes are known for both the recovery and oxidizing gases [16-17].

As mentioned above, pure SnO_2 is an n-type semiconductor due to the existence of the native donor levels. However, pure SnO_2 exhibits low sensitivity and poor selectivity as well as high electrical resistance. In order to modify or control the chemical and physical properties of the SnO_2, introduction of noble metals and different additives is performed. Therefore, it is necessary to add appropriate dopant in pure metal oxide for improving the gas sensing properties. Dopants can affect the main parameters of SnO_2 based sensor important to gas sensing applications. Sensitivity, selectivity and stability can vary depending on the type and quantity of dopants. Inhibiting of SnO_2 grain growth, modifying the electron Debye length and modifying the gas-surface interactions can be also controlled by additives [18-20].

The aims of the present paper are development of technology, manufacturing and investigation of solid-state hydrogen peroxide vapors sensor made of semiconductor metal oxide nanostructured SnO_2<Co> film.

2. Sensors Preparation and Material Characterization

Ceramic targets made of metal oxide SnO_2 doped with 2 at.% Co were synthesized by the method of solid-phase reaction in the air [21]. The compacted samples SnO_2<Co> were exposed to thermal treatment in the programmable furnace Nabertherm, HT O4/16 with the controller of C 42. The annealing was carried out at 500°C, 700°C, 1000°C and 1100°C consecutively, soaking at each temperature during 5 h (Table 1). Then the compositions were subjected to mechanical treatment in the air in order to eliminate surface defects. Thus, smooth parallel targets with a diameter ~ 40 mm and thickness ~ 2 mm were prepared (Fig. 1).

Table 1. The annealing steps of SnO_2 doped with 2 at.% Co ceramic target.

No.	Annealing temperature, ^{0}C	Annealing time, hour
1.	25 - 500	4
2.	500	5
3.	500 - 700	1
4.	700	5
5.	700 - 1000	1
6.	1000	5
7.	1000 - 1100	1
8.	1100	5
9.	1100 - 25	10

Chemical composition of prepared SnO_2<Co> targets was studied using Niton™ XL3t GOLDD+

XRF Analyzer. The results of this investigation have shown that the real content of cobalt's atoms on the surface of the prepared ceramic targets was equal to 1.3at.%. So, ceramic targets with compositions of $Sn_{0,987}Co_{0,013}O_2$, were synthesized.

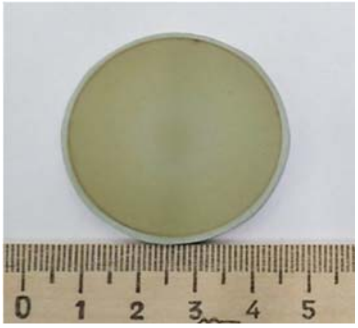

Fig. 1. The photo of the ceramic target based on SnO_2 doped with 2 at.% Co (with cm unit).

Prepared semiconductor SnO_2<Co> targets were used for deposition of nanosized films on Multi-Sensor-Platforms using the high-frequency magnetron sputtering method. The platform integrates a temperature sensor (Pt 1000), a heater and interdigitated platinum electrodes on a ceramic substrate. The heater and temperature sensor were covered with an insulating glass layer. Gas sensitive layer made of $Sn_{0,987}Co_{0,013}O_2$ was deposited onto the non-passivated electrode structures. That way the Multi-Sensor-Platform was converted into gas sensor (Fig. 2).

The following working conditions of the high-frequency magnetron sputtering were chosen: the power of the magnetron generator unit was 60 W; the substrate temperature during the sputtering was 200 °C and the duration of the sputtering process was equal to 20 minutes. The sensing device was completed through the ion-beam sputtering deposition of palladium catalytic particles (the deposition time ~ 3 seconds). Further annealing of the manufactured structures in the air was carried out at temperature of 250 °C during 2 hours to obtain homogeneous films and eliminate mechanical stresses.

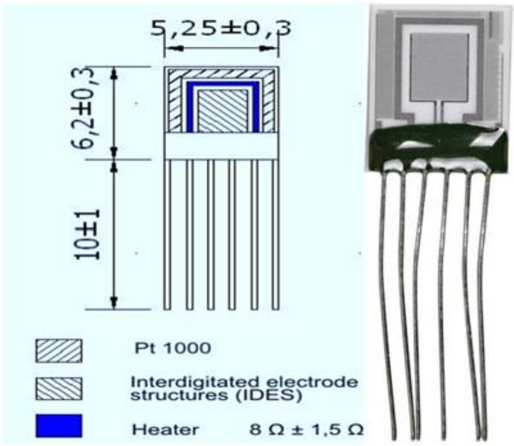

Fig. 2. The schematic diagram (with mm unit) and photo of the Multi-Sensor-Platform.

The thickness of the deposited doped metal oxide film was measured by the Alpha-Step D-100 (KLA Tencor) profiler. The result of study of the film - substrate transition profile is shown in Fig. 3. The thickness of the SnO_2<Co> film was equal to 138 nm.

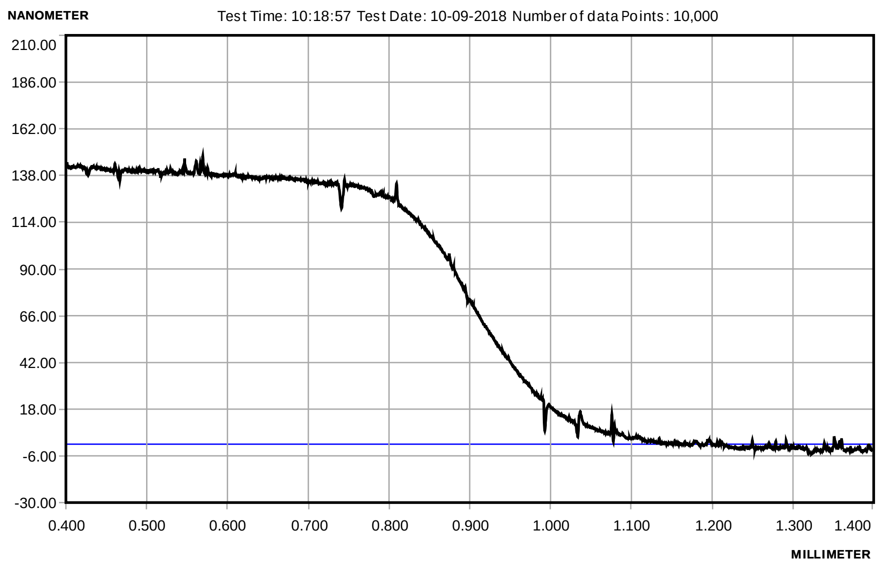

Fig. 3. The $Sn_{0,987}Co_{0,013}O_2$ film thickness measurement result.

The sensitivity to different gases depends on the microstructure of the sensing material, especially on the porosity and grain size [22-25]. The morphology of the deposited Co-doped SnO_2 films was studied by scanning electron microscopy using Mira 3 LMH (Tescan). The average size of nanoparticles was approximately equal to 18.7 nm (Fig. 4).

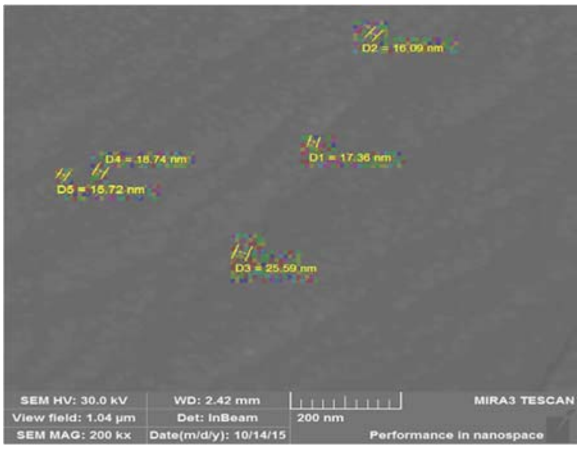

Fig. 4. The SEM image of the $Sn_{0,987}Co_{0,013}O_2$ film.

3. Experimental Results and Discussion

It is known, that the sensing mechanism of n-type (SnO_2<Co> is an n-type semiconductor metal oxide) semiconductor gas sensors can be explained by modulation model of surface electron depletion layer or modulation of inter-grain barrier. Commonly, when the doped SnO_2<Co> layer is exposed to air, ambient oxygen molecules or atoms adsorb on the sensor surface and capture the conduction-band electrons to become chemisorbed active ionic species of oxygen. Thus, an electron depletion layer is formed near the SnO_2<Co> sensor surface and we have an increasing in the resistance of semiconductor resistive thin film. When the target oxidizing gas molecules (H_2O_2) are introduced to surface of the sensor, there are dissociated on the surface of semiconductor and are supplemented by additional oxygen atoms. These additional oxygen atoms capture the conduction-band electrons again resulting to increase the resistance of the SnO_2<Co> thin film. So, with the presence of H_2O_2, we have an increasing or changing in resistance of sensing layer.

The gas sensing properties of the prepared sensors under the influence of H_2O_2 vapors were investigated using an internally developed and computer-controlled static gas sensor test system [26]. The sensitivity of the SnO_2<Co> sensor to the different concentrations of H_2O_2 vapors were measured at different heating temperatures of gas-sensitive film. The sensor response was determined as the ratio of R_{gas}/R_{air}, where R_{gas} is the resistance in the presence of target gas in the air and R_{air} is the resistance in the air without target gas.

Our measurements showed that the SnO_2<Co> sensor exhibited a sufficient sensitivity to H_2O_2 vapors even at room temperature. For example, the resistance of the sensor increases by 2.2 and 8 times at presence of H_2O_2 vapors with the concentration of 3.5 ppm and 105 ppm, respectively (response times were 10 and 5 minutes, respectively) at operating temperature of 25 ºC. Typical results of measurements of changes in the resistance of the SnO_2<Co> sensor at low operating temperatures are presented in Fig. 5. As we can see, there remains the problem of restoring the sensor resistance to its original values at such operating temperatures. Additional heating is required to overcome this problem.

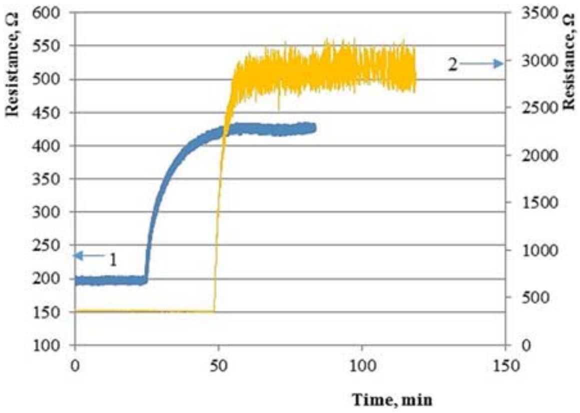

Fig. 5. The response-recovery curves of SnO_2<Co> sensor observed under the influence of 3.5 ppm (1) and 105 ppm (2) of H_2O_2 vapors measured at 25ºC operating temperature.

The dependence of the resistance of nanostructured SnO_2<Co> film in the air on temperature was studied. It is known that its resistance decreases when bulk semiconductor is heated, which is due to the increasing of the concentration of free carrier in the conduction band. In case of thin films, the situation is somewhat different. The problem is that when the temperature of thin film increases its resistance decreases and starting at a certain temperature rises again and in some cases reaching its saturation value. The dependence of the resistance of the nanostructured SnO_2<Co> film on temperature in the air is presented in Fig. 6.

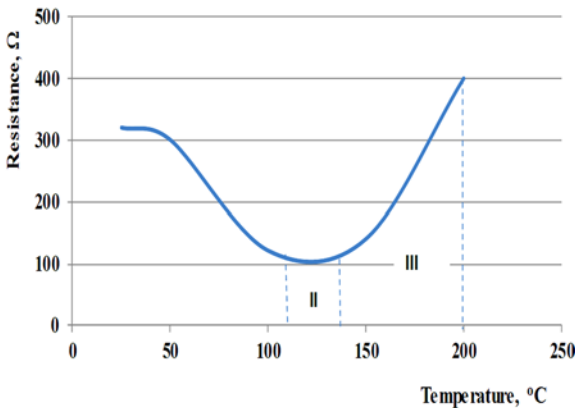

Fig. 6. The dependence of resistance of nanostructured SnO_2<Co> film in the air on temperature.

As can see, the temperature dependence of the film's resistance shows so-called three-region behavior. The resistance drop in the first region is due to the generating of electrons in the conduction band as a result of thermal excitation, as in ordinary bulk semiconductors. The temperature effect in the second region is rather small and there is a competition between electrons generation process and the surface adsorption of active oxygen. So, there is a balance between the thermal excitation and oxygen adsorption processes. The increasing of the resistance in the third region is due to the increasing of adsorption rate of active oxygen on the surface of the thin film. So, the operating temperature of the sensor should be selected in the region where the oxygen adsorption and desorption processes are performed faster and intensely.

The responses of SnO_2<Co> sensor to the H_2O_2 vapors at different operating temperatures were also measured. Even with such a low concentration of H_2O_2 vapors as 875 ppb, the responses of the sensor were 2.8 and 2.15 at 100 and 150 °C operating temperature, respectively (Fig. 7a).

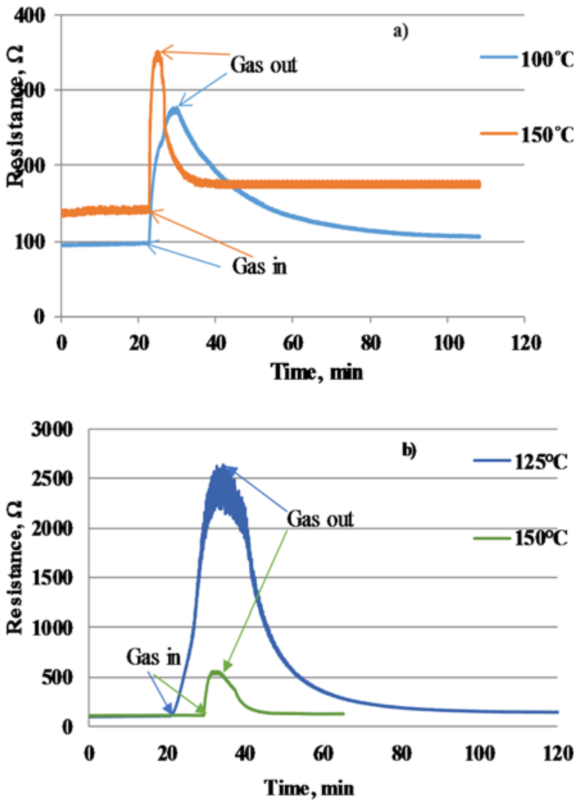

Fig. 7. The response-recovery curves of SnO_2<Co> sample observed under the influence of 875 ppb (a) and 3.5 ppm (b) of H_2O_2 vapors measured at different operating temperatures.

The response times were equal to 4.5 and 1.08 minutes at 100 and 150 °C operating temperature, respectively. The recovery times were equal to 41.8 and 6 minutes at 100 and 150 °C operating temperature, respectively. So, the response value of SnO_2<Co> sensor was higher at 75, 100 and 125 °C operating temperatures than that of at 150 °C operating temperature, but from the point of view of high performance the 150 °C was chosen as an optimal operating temperature. This conclusion is confirmed by the results of measurements of the SnO_2<Co> sensor sensitivity to H_2O_2 vapors with 3.5 ppm concentration at different operating temperatures (Fig. 7b and Fig. 8).

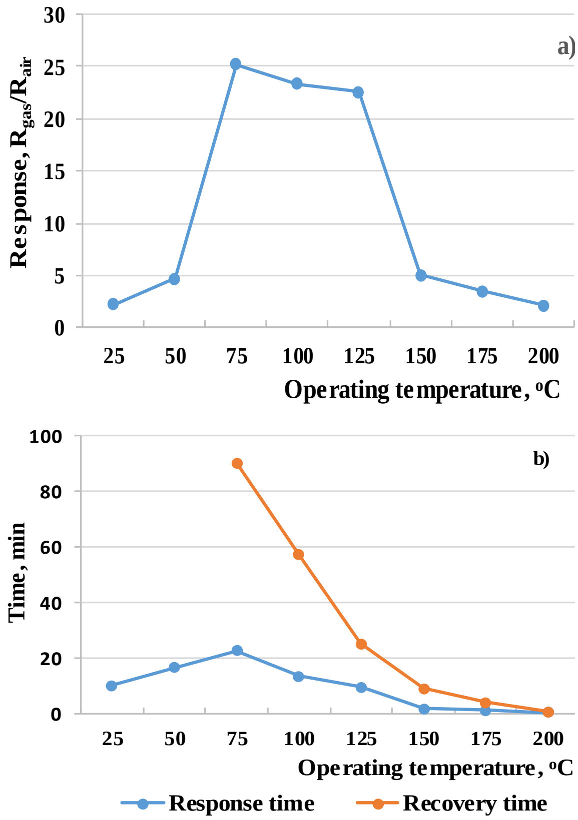

Fig. 8. a) The *dependence* of the *response* of the SnO_2<Co> sensor on the operating temperature at the 3.5 ppm H_2O_2 vapors; b) The dependences of the sensor response and recovery times on the operating temperature.

Despite the fact that the sensor response at 125 °C is higher than at 150 °C, the response time is almost 6 times, and the recovery time is 3 times less. As seen from Fig. 8b, further increase of the gas-sensitive film temperature leads to a decrease of response and recovery times.

The sensitivity curves of SnO_2<Co> sample observed under the influence of different concentrations of H_2O_2 vapors measured at 150 °C operating temperature are presented in Fig. 9. By changing of H_2O_2 vapors concentration from 875 ppb to 105 ppm the sensitivity increases from 2.15 to 290.

The *dependence* of *response* on the H_2O_2 vapors concentration at 150 °C operating temperature is presented in Fig. 10. The dependence has almost linear character that will allow not only to detect low concentrations of H_2O_2 vapors but also to accurately measure the concentration.

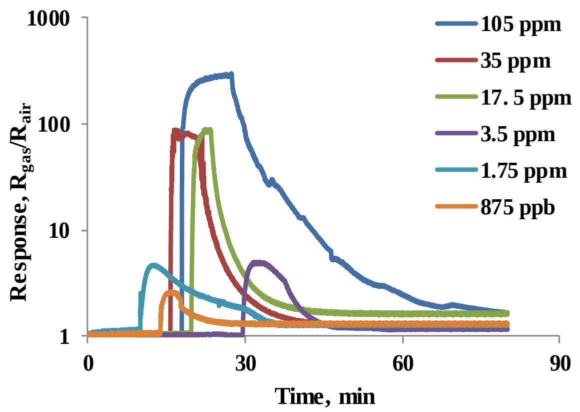

Fig. 9. The sensitivity curves of SnO_2<Co> sensor observed under the influence of different concentrations of H_2O_2 vapors at 150°C operating temperature.

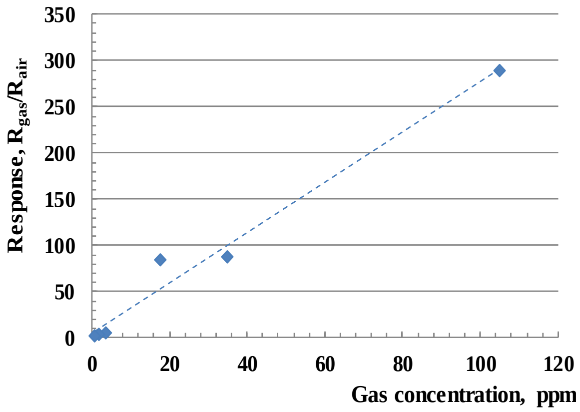

Fig. 10. The *dependence* of *response* of SnO_2<Co> sensor on the H_2O_2 vapors concentration.

The dependences of the sensor response and recovery time on the H_2O_2 vapors concentration at 150 °C operating temperature have also been eliminated (Fig. 11). As we see, with the increasing in H_2O_2 vapors concentration, the response and recovery times do not change significantly, but the response times are relatively small compared to the recovery times.

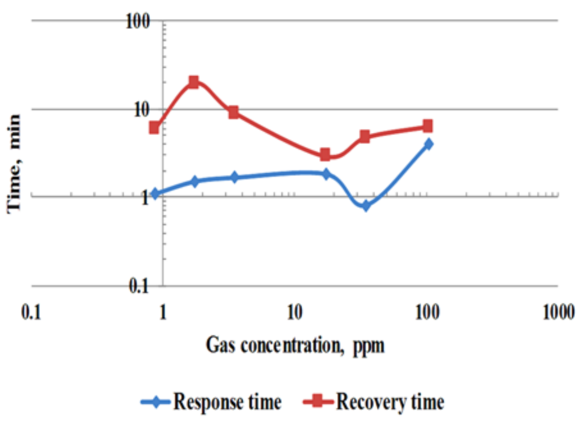

Fig. 11. The dependences of the sensor response and recovery time on the H_2O_2 vapors concentration.

The sensing results obtained in this study at 150 °C operation temperature are presented in Table 2. The sensor made of doped metal oxide SnO_2<Co> has shown sensitivity to 875 ppb H_2O_2 concentration and even in such low concentrations the resistance has changed more than twice. The sensitivity of the doped SnO_2<Co> sensors varies approximately 300 times in relatively high concentrations (105 ppm) of H_2O_2 vapors, which is also a reliable result. The response times are mainly less than two minutes which is really short for this type of sensor, but the recovery times compared to the response times are longer.

Table 2. Sensing performance of the SnO_2<Co> sensor tested at 150 °C operating temperature.

SnO_2<Co> sensor			
H_2O_2 vapors concentration, ppm	**Response, R_{gas}/R_{air}**	**Response time, min**	**Recovery time, min**
105	290	4.1	6.3
35	87.43	0.8	4.75
17.5	84.5	1.83	2.88
3.5	5	1.66	9
1.75	4.22	1.5	19.5
0.875	2.15	1.08	6

4. Conclusions

We have developed and characterized doped metal oxide SnO_2<Co> thin film sensor structure made using high frequency magnetron sputtering method for H_2O_2 vapors sensing. The chemical analysis showed that the gas sensitive film had a $Sn_{0,987}Co_{0,013}O_2$ composition. The SnO_2<Co> film thickness was equal to 138 nm. The average size of nanoparticles was equal to 18.7 nm. The sensitivity of the sensors was improved by sputtering palladium catalytic particles on the surface of the sensing layer. The gas sensing properties of the prepared SnO_2<Co> sensors were investigated under the influence of the different concentration of H_2O_2 vapors at different operation temperatures. The sensor made of SnO_2<Co> has sensitivity to 3.5 ppm H_2O_2 vapors even at room temperature. The *dependence* of *response* on the H_2O_2 vapors concentration has almost linear characteristic at 150 °C operating temperature. The sensor made of SnO_2<Co> exhibited high sensitivity, fast response and recovery behavior at the ppb level of H_2O_2 vapors.

Acknowledgements

This research was supported by the DecoComp project which funded by the Swiss National Science Foundation FNSNF under the framework of SCOPES.

References

[1]. G. Yu, W. Wu, X. Pan, Q. Zhao, X. Wei, Q. Lu, High sensitive and selective sensing of hydrogen peroxide

released from pheochromocytoma cells based on Pt-Au bimetallic nanoparticles electrodeposited on reduced graphene sheets, *Sensors*, Vol. 15, Issue 2, 2015, pp. 2709-2722.

[2]. J. Agrisuelas, M. González-Sánchez, E. Valero, Hydrogen peroxide sensor based on in situ grown Pt nanoparticles from waste screen-printed electrodes, *Sensors and Actuators B: Chemical*, Vol. 249, Issue 10, 2017, pp. 499–505.

[3]. D. Lee, S. Choi, Y. Byun, Room temperature monitoring of hydrogen peroxide vapor using platinum nanoparticles-decorated single-walled carbon nanotube networks, *Sensors and Actuators B: Chemical*, Vol. 256, Issue 3, 2018, pp. 744–750.

[4]. B. Patella, R. Inguanta, S. Piazza, C. Sunseri, A nanostructured sensor of hydrogen peroxide, *Sensors and Actuators B: Chemical*, Vol. 245, Issue 6, 2017, pp. 44–54.

[5]. A. L. Verma, S. Saxena, G. S. S. Saini, V. Gaur, V. K. Jain, Hydrogen peroxide vapor sensor using metal-phthalocyanine functionalized carbon nanotubes, *Thin Solid Films*, Vol. 519, Issue 22, 2011, pp. 8144–8148.

[6]. V. M. Aroutiounian, Properties of hydrogen peroxide solid-state sensors made from nanocrystalline materials, *Sensors and Transducers*, Vol. 223, Issue 7, 2018, pp. 9-21.

[7]. D. O'Sullivana, K. C. Silwal, A. S. McNeill, V. Treadawayc, B. G. Heikes, Quantification of gas phase hydrogen peroxide and methyl peroxide in ambient air: Using atmospheric pressure chemical ionization mass spectrometry with O_2^-, and $O_2^-(CO_2)$ reagent ions, *International Journal of Mass Spectrometry*, Vol. 424, Issue 1, 2018, pp. 16–26.

[8]. B. Puértolas, A. K. Hill, T. Garcíaa, B. Solsonac, L. Torrente-Murciano, In-situ synthesis of hydrogen peroxide in tandem with selective oxidation reactions: A mini-review, *Catalysis Today*, Vol. 248, Issue 6, 2015, pp. 115–127.

[9]. P. Kačer, J. Švrček, K. Syslová, J. Václavík, D. Pavlík, J. Červený, M. Kuzma, Vapor phase hydrogen peroxide – method for decontamination of surfaces and working areas from organic pollutants, in: Organic pollutants ten years after the Stockholm Convention – environmental and analytical update, *InTech,* Chapter 17, 2012, pp. 399-430.

[10]. S. Corveleyn, G. M. R. Vandenbossche, J. P. Remon, Near-infrared (NIR) monitoring of H_2O_2 vapor concentration during vapor hydrogen peroxide (VHP) sterilization, *Pharmaceutical Research*, Vol. 14, Issue 3, 1997, pp. 294-298.

[11]. P. Salazar, V. Rico, A. R. González-Elipe, Non-enzymatic hydrogen peroxide detection at NiO nanoporous thin film- electrodes prepared by physical vapor deposition at oblique angles, *Electrochimica Acta*, Vol. 235, Issue 5, 2017, pp. 534–542.

[12]. B. P. Garreffia, M. Guoa, N. Tokranovab, N. C. Cadyb, J. Castracaneb, I. A. Levitskyc, Highly sensitive and selective fluorescence sensor based on nanoporous silicon-quinoline composite for trace detection of hydrogen peroxide vapors, *Sensors and Actuators B: Chemical*, Vol. 276, Issue 12, 2018, pp. 466-471.

[13]. F. I. Bohrer, C.N. Colesniuc, J. Park, I. K. Schuller, A. C. Kummel, W. C. Trogler, Selective detection of vapor phase hydrogen peroxide with phthalocyanine chemiresistors, *Journal of the American Chemical Society*, Vol. 130, Issue 12, 2008, pp. 3712-3713.

[14]. J. N'Diaye, S. Poorahong, O. Hmam, R. Izquierdo, M. Siaj, Facile synthesis rhodium nanoparticles decorated single layer graphene as an enhancement hydrogen peroxide sensor, *Journal of Electroanalytical Chemistry*, Vol. 789, Issue 3, 2017, pp. 85–91.

[15]. T. A. Miller, S. D. Bakrania, C. Perez, M. S. Wooldridge, Nanostructured tin dioxide materials for gas sensor applications, in Functional Nanomaterials, Eds. K. E. Geckeler, E. Rosenberg, *American Scientific Publishers*, Chapter 30, 2006, pp. 1-24.

[16]. A. Klein, C. Korber, A. Wachau, F. Sauberlich, Y. Gassenbauer, S. P. Harvey, D. E. Proffit, T. O. Mason, Transparent conducting oxides for photovoltaics: manipulation of fermi level, work function and energy band alignment, *Materials*, Vol. 3, Issue 11, 2010, pp. 4892-4914.

[17]. A. Dey, Semiconductor metal oxide gas sensors: A review, *Materials Science and Engineering B,* Vol. 229, Issue 3, 2018, pp 206-217.

[18]. V. M. Aroutiounian, V. M. Arakelyan, E. A. Khachaturyan, G. E. Shahnazaryan, M. S. Aleksanyan, L. Forro, A. Margez, K. Hernadi, Z. Nemeth, Manufacturing and investigations of i-butane sensor made of SnO_2/multiwall-carbon-nanotube nanocomposite, *Sensors and Actuators B: Chemical*, Vol. 173, Issue 10, 2012, pp. 890-896.

[19]. W. Zhao, J. Jin, H. Wu, S. Wang, C. Fneg, S. Yang, Y. Ding, Electrochemical hydrogen peroxide sensor based on carbon supported Cu@Pt core-shell nanoparticles, *Materials Science and Engineering C*, Vol. 78, Issue 9, 2017, pp. 185–190.

[20]. G. Korotcenkov, Metal oxide composites in conductometric gas sensors: Achievements and challenges, *Sensors and Actuators B: Chemical,* Vol. 244, Issue 6, 2017, pp. 182-210.

[21]. V. M. Aroutiounian, V. M. Arakelyan, M. S. Aleksanyan, G. E. Shahnazaryan, A. G. Sayunts, B. Joost, Co-doped SnO_2 sensor for detection of hydrogen peroxide vapors, in *Proceedings of the 4th International Conference on Sensors Engineering and Electronics Instrumentation Advances (SEIA'18),* Amsterdam, The Netherlands, 19-21 September 2018, pp. 49-52.

[22]. A. Rothschild, Y. Komem, The effect of grain size on the sensitivity of nanocrystalline metal-oxide gas sensors, *Journal of Applied Physics*, Vol. 95, Issue 11, 2004, pp. 6374-6382.

[23]. C. Wang, L. Yin, L. Zhang, D. Xiang, R. Gao, Metal oxide gas sensors: sensitivity and influencing factors, *Sensors*, Vol. 10, Issue 3, 2010, pp. 2088-2106.

[24]. M. S. Aleksanyan, V. M. Arakelyan, V. M. Aroutiounian, G. E. Shahnazaryan, Investigation of gas sensor based on In_2O_3:Ga_2O_3 film, *Journal of Contemporary Physics (Armenian Academy of Sciences)*, Vol. 46, Issue 2, 2011, pp. 86-92.

[25] Sh. Gong, J. Liu, J. Xia, L. Quan, H. Liu, D. Zhou, Gas sensing characteristics of SnO_2 thin films and analyses of sensor response by the gas diffusion theory, *Materials Science and Engineering B,* Vol. 164, Issue 2, 2009, pp. 85-90.

[26]. Z. Adamyan, A. Sayunts, V. Aroutiounian, E. Khachaturyan, M. Vrnata, P. Fitl, J. Vlček. Nanocomposite sensors of propylene glycol, dimethylformamide and formaldehyde vapors, *Journal of Sensors and Sensor Systems*, Vol. 7, Issue 1, 2018, pp. 31-41.